ELSEVIER

Atmospheric Environment 38 (2004) 5555–5566

ATMOSPHERIC ENVIRONMENT

www.elsevier.com/locate/atmosenv

Modelling airborne concentration and deposition rate of maize pollen

Nathalie Jarosz*, Benjamin Loubet, Laurent Huber

Institut National de Recherche Agronomique (INRA), UMR-EGC, 78850 Thiverval-Grignon, France

Received 26 February 2004; received in revised form 8 June 2004; accepted 17 June 2004

Abstract

The introduction of genetically modified (GM) crops has reinforced the need to quantify gene flow from crop to crop. This requires predictive tools which take into account meteorological conditions, canopy structure as well as pollen aerodynamic characteristics. A Lagrangian Stochastic (LS) model, called SMOP-2D (Stochastic Mechanistic model for Pollen dispersion and deposition in 2 Dimensions), is presented. It simulates wind dispersion of pollen by calculating individual pollen trajectories from their emission to their deposition. SMOP-2D was validated using two field experiments where airborne concentration and deposition rate of pollen were measured within and downwind from different sized maize (*Zea mays*) plots together with micrometeorological measurements. SMOP-2D correctly simulated the shapes of the concentration profiles but generally underestimated the deposition rates in the first 10 m downwind from the source. Potential explanations of this discrepancy are discussed. Incorrect parameterisation of turbulence in the transition from the crop to the surroundings is probably the most likely reason. This demonstrates that LS models for particle transfer need to be coupled with air-flow models under complex terrain conditions.

Keywords: Atmospheric dispersion; Lagrangian model; Turbulence; Particles; *Zea mays*

1. Introduction

Pollen dispersion has been the subject of an increasing number of studies since the introduction of genetically modified (GM) crops because of the need to maintain seed purity. In Europe, the main objective for maize (*Zea mays*) crops has been to quantify gene flow from transgenic to non-transgenic crops as there is no risk of hybridisation with its wild relative, teosinte (White and Doebley, 1998; Matsuoka et al., 2002) because it does not grow there. However, teosinte does grow in Central America and the risk of hybridisation has become a subject of scientific inquiry (Doebley, 1990; Baltazar and Schoper, 2002).

Many models of pollen dispersion have been based on observed levels of outcrossing on target plants in the vicinity of an emitting source plot (Lavigne et al., 1998; Klein, 2000). Such studies can give direct estimates of outcrossing rates, but are of limited use as predictive tools because they are only valid for the meteorological conditions found during the experiments. A few models of atmospheric pollen dispersion based on concentration and deposition measurement exist (McCartney et al., 1985; Jackson and Lyford, 1999), but to our knowledge, none has been applied to maize. In this study, we evaluate an alternative and complementary approach using a Lagrangian Stochastic (LS) model to simulate

*Corresponding author. Present address. Institut National de Recherche Agronomique (INRA), EPHYSE, BP 81, 33883 Villenave d'Ornon, France.

E-mail address: njarosz@bordeaux.inra.fr (N. Jarosz).

1352-2310/$ - see front matter
doi:10.1016/j.atmosenv.2004.06.027

wind dispersion of maize pollen. The model, called SMOP-2D (Stochastic Mechanistic model for Pollen dispersion and deposition in 2 Dimensions), predicts pollen concentration and deposition rate downwind from an emitting field. SMOP-2D is a mechanistic model that considers atmospheric turbulence, pollen aerodynamic characteristics and canopy structure. It also includes an empirical parameterisation of the turbulence field for heterogeneous landscapes. These features allow the investigation of contrasting scenarios. LS models have proved to be accurate for calculating the dispersion of atmospheric gases (Wilson and Sawford, 1996). They have been successfully extended to simulate heavy particle dispersion (Walklate, 1986; Reynolds, 1999; Wilson, 2000) and have been used to estimate fungal spore release rates (Aylor and Flesch, 2001).

Here we validate the LS model SMOP-2D by comparing calculated concentrations and deposition rates with those measured during field experiments conducted in 2000 (Jarosz et al., 2003) and 2001 (Jarosz, 2003).

2. Material and methods

2.1. Model

SMOP-2D is an LS model in 2 dimensions (horizontal downwind (x) and vertical (z)) that simulates the wind dispersion of pollen grains by calculating a large number of individual trajectories. SMOP-2D is a version of the LS model initially developed for atmospheric ammonia dispersion that was adapted for pollen dispersion (Loubet, 2000), and is very similar to the spore dispersal model reported by Aylor and Flesch (2001). Pollen can be treated as a passive scalar, with a settling velocity V_s added to the vertical velocity component, provided that the size is in the range $20\,\mu\text{m} \leqslant \text{diameter} \leqslant 300\,\mu\text{m}$ (Wilson, 2000). The displacement of individual pollen grains is calculated using the following two-dimensional joint stochastic differential equations:

$$\mathrm{d}u = a_u\,\mathrm{d}t + b_u\,\mathrm{d}\xi_u, \quad \mathrm{d}x = u\,\mathrm{d}t,$$

$$\mathrm{d}w = a_w\,\mathrm{d}t + b_w\,\mathrm{d}\xi_w, \quad \mathrm{d}z = (w - V_s)\,\mathrm{d}t, \tag{1}$$

u and w are the horizontal and vertical air velocity components; a_u, b_u, a_w and b_w are the Langevin coefficients; and $\mathrm{d}\xi_u$ and $\mathrm{d}\xi_w$ are random numbers drawn from Gaussian distributions with mean zero and variance $\mathrm{d}t$. The Langevin coefficients are functions of the average horizontal (U) and vertical (W) components of air velocity; the horizontal (σ_u^2) and vertical (σ_w^2) Eulerian velocity variances; the shear stress ($\overline{u'w'}$), and the Lagrangian velocity timescale (T_L). Over a flat homogeneous terrain, W is assumed to be zero. The coefficients a_u, b_u, a_w and b_w are determined from the well-mixed criterion and the Kolmogorov similarity hypothesis, under stationary and horizontally homogeneous flow (Rodean, 1996; Thomson, 1987; Aylor and Flesch, 2001). In this study, these coefficients are those detailed by Wilson and Flesch (1997) for models preserving the mean direction of the fluctuating velocity vector, which corresponds to Thomson's model (1987). They are therefore not given here. Due to gravitational forces and inertia, heavy particles do not follow the fluid trajectories exactly (Sawford and Guest, 1991). This effect is taken into account by reducing the fluid velocity time scale along a particle trajectory, τ_p, compared to that of a fluid trajectory, T_L (Sawford and Guest, 1991):

$$\tau_p = \frac{T_L}{\sqrt{1 + \left(\frac{\beta V_s}{\sigma_w}\right)^2}}, \tag{2}$$

where β is an empirical dimensionless constant. In this study β was taken to be 3 (Snyder and Lumley, 1971). But, the value of β for particle dispersion is still subject to debate (see e.g. Wilson, 2000).

2.1.1. Turbulence field

The parameterisation of the turbulence for horizontally homogeneous conditions is described in Loubet (2000), and includes vertical profiles of U, W, σ_u^2, σ_w^2, $\overline{u'w'}$ and T_L. A simple empirical parameterisation of the turbulent field in the transition zone between two different canopies was chosen. The transition zone was defined as the location between the upwind position, x_{upwind}, where the turbulent field is defined by the characteristics of the upwind canopy, and the downwind position, x_{downwind}, where the field is defined by the downwind canopy (Fig. 1). At any position, x, within this zone, each vertical profile of a given turbulent characteristic was interpolated between the upwind and downwind equilibrium profiles using a 3rd degree polynomial P. To simplify the expression of the polynomial, a normalised distance X was used:

$$X = \frac{x - x_{\text{upwind}}}{x_{\text{downwind}} - x_{\text{upwind}}}. \tag{3}$$

The polynomial was defined as $P(X) = -2X^3 + 3X^2$. This ensured the continuity of the profiles and their derivatives over the transition zone: it satisfied four constraints: $P(0) = 0, P(1) = 1$ and $P'(0) = P'(1) = 0$. Mass conservation was ensured by calculating W as the integral over z of the derivative of U over $x(-\mathrm{d}U/\mathrm{d}x)$. This parameterisation allows the most influencing parameters to vary realistically over the transition zone. However, the parameterisation of $\overline{u'w'}$ profiles may not be ideal, as these profiles should increase at the transition and decrease afterwards (Bradley, 1968), whereas here the profiles change smoothly from upwind to downwind. The parameterisation of the flow in the transition zone was designed to

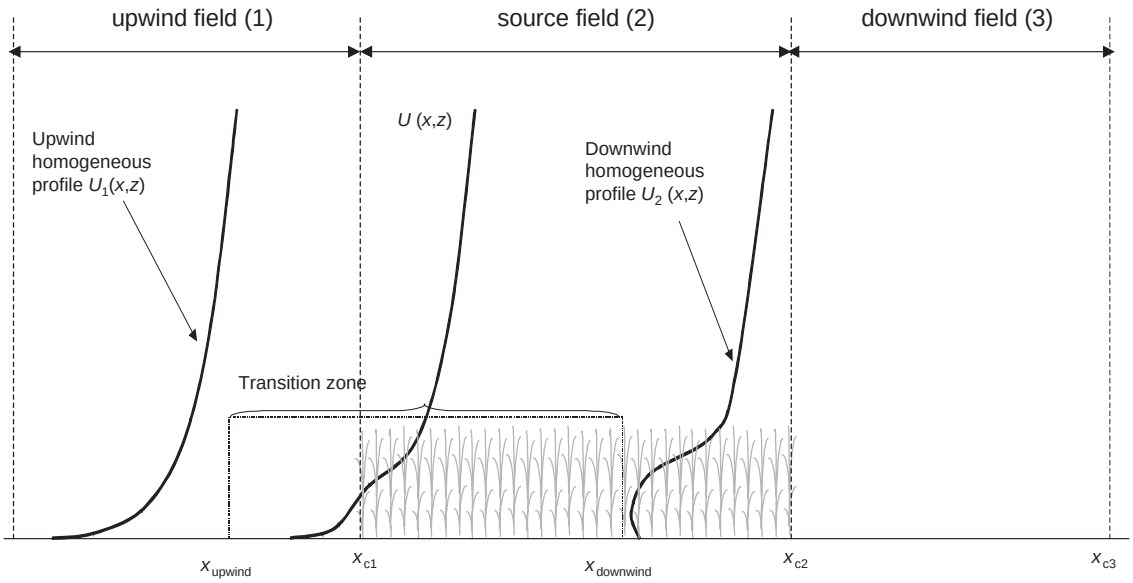

Fig. 1. Wind speed profiles illustrating the parameterisation of the turbulent exchanges in the transition zone between two adjacent canopies. Interpolation is made between equilibrium profiles in contiguous fields. Here x_{ci} is the downwind fetch of the field i, and x_{upwind} and $x_{downwind}$ are the upwind and downwind distance influenced by the roughness change.

get a realistic but simple turbulence field. It was therefore not considered necessary to add more complexity to the stochastic model. Hence we did not include the horizontal derivatives in the coefficients a_u, b_u, a_w and b_w as should be done under non-homogeneous turbulence (Leuzzi and Monti, 1998). However, the effect of including these derivatives was evaluated: it generated unsteadiness in the trajectories, but did not show great differences in concentration and deposition rates, when compared with the effect of a modification in the turbulence field.

2.1.2. Model parameters and input variables

SMOP-2D considers canopy and pollen characteristics, and micrometeorological variables (Table 1). The canopy parameters for each field are: the downwind fetch (x_c); height (h_c), roughness length (z_0); displacement height (d); and the leaf area density (LAD), made up of the horizontal and vertical projections (LAD^x and LAD^z). Pollen aerodynamic characteristics were accounted for using a Gaussian distribution of the settling velocity V_s. Unless otherwise stated, a mean of $0.31\,m\,s^{-1}$ and a standard deviation of $0.08\,m\,s^{-1}$ were taken for the distribution of V_s, which is consistent with Di-Giovanni et al. (1995), although smaller means have been measured by others (Aylor, 2002; Jarosz, 2003). The simulations were carried out over a horizontal distance, x_D, and vertical height, z_D. The area was divided into a grid with N_x horizontal and N_z vertical elements for concentration estimates. The grid in the maize canopy had more tightly spaced vertical layers (N_h).

2.1.3. Concentration and deposition

The model outputs were pollen concentration (C); deposition rate to the ground (D^g); and deposition rate to vegetation surfaces (D^v). The concentration C was calculated for any point (i, j) of the grid ($i = 1$ to N_x and $j = 1$ to N_z) as Flesch (1995):

$$C(i,j) = V_{source} \times \frac{1}{N_p} \sum_{n=1}^{N_p} T_n(i,j)/V(i,j), \tag{4}$$

where V_{source} is the volume of the source, N_p is the number of trajectories, and T_n is the residence time of particle n in the grid division of volume $V(i,j)$.

Deposition within the canopy was expressed as the sum of the contribution due to gravitational settling and the contribution due to inertial impaction (Legg and Powell, 1979). The probability that pollen deposits on the vegetation (D^v) or on the ground (D^g) over a time step dt was calculated according to Aylor and Flesch (2001). The deposition rate either at the ground or on the vegetation in the horizontal grid location i ($i = 1$ to N_x) was specified as

$$D^{g,v}(i) = V_{source} \times \frac{1}{N_p} \sum_{n=1}^{N_p} D_n^{g,v}(i)/A(i), \tag{5}$$

where $D_n^{g,v}$ is the probability that the pollen grain n deposits on the ground or vegetation and A is the area available for deposition at distance i.

Table 1
Main input parameters of the SMOP-2D model, with units and typical values used in this study

Symbol	Parameter	Units	Typical values used in this study
Canopy			
x_c	Downwind fetch of the field	m	20–200
h_c	Canopy height	m	0.1–0.2 and 2.2–2.3
z_0	Roughness length	m	$0.1 \times h_c$
d	Displacement height	m	$0.7 \times h_c$
L_f	Leaf size	m	0.01–0.05
x_{upwind}	Upwind distance influenced by the roughness change	m	$3-10 \times h_c$
$x_{downwind}$	Downwind distance influenced by the roughness change	m	$10-20 \times h_c$
LAD(z)	Leaf Area Density as a function of z	$m^2\,m^{-3}$	0.5–2.5
$LAD_x(z)$	Fraction of the plant projected onto horizontal plan	$m^2\,m^{-3}$	0–1.3
$LAD_z(z)$	Fraction of the plant projected onto vertical plan	$m^2\,m^{-3}$	0–0.8
Total Area			
$0-x_D$	Horizontal size of the total area	m	130 or 254
$0-z_D$	Vertical size of the total area	m	10
Grid			
N_x	Number of horizontal grid divisions	—	100
N_z	Number of vertical grid divisions	—	20
N_h	Number of vertical layers within the source	—	10
Source			
N_p	Number of pollen grains released	—	10 000
$x_{Smin} - x_{Smax}$	Horizontal limits of the source	m	0–20 or 0–24
$z_{Smin} - z_{Smax}$	Vertical limits of the source	m	2.0–2.3 or 2.3–2.5
S_{dens}	Release rate of the source	grains $m^{-2}\,s^{-1}$	1
Particle			
V_s	Mean settling velocity of the pollen	$m\,s^{-1}$	0.31
std V_s	Standard deviation of settling velocity	$m\,s^{-1}$	0.08
β	Empirical constant in the Lagrangian timescale	—	3
Turbulence			
L	Monin–Obukhov length	m	−2 to −100
U_{ref}	Mean wind speed at a reference height z_{ref}	$m\,s^{-1}$	1.72–10.81
z_{ref}	The reference height at which wind speed is given	m	50
C_0	Universal Lagrangian velocity structure constant	—	3
$\sigma_u/u*$	Ratio of along—wind square root velocity variance to $u*$	—	3.1
$\sigma_w/u*$	Ratio of vertical square root velocity variance to $u*$	—	1.4
γ	Attenuation coefficient for mean wind speed in the canopy	—	2.5
$T_L u*/h_c$	Ratio of the fluid Lagrangian time scale (T_L times $u*$ to h_c within the canopy)	—	0.3
$\Delta t/T_L$	Time step for the particle trajectory as a ratio of T_L	—	0.01

2.2. Model validation

2.2.1. Experimental data

The model outputs were compared with measurements recorded during two field experiments one at Montargis and the other at Grignon, France, in 2000 and 2001, respectively (Jarosz et al., 2003; Jarosz, 2003). Vertical profiles of pollen concentration were measured at $x = 3$ and 10 m downwind from a 20×20 m maize plot at Montargis and two 24×42 m maize plots at Grignon. Pollen deposition rates were measured between $x = 1$ and 32 m in Montargis and $x = 1$ and 200 m in Grignon. Micrometeorological measurements were made during the entire pollination period. The plots were isolated from other possible sources of maize pollen: at Montargis, the plot was surrounded by bare soil, and at Grignon, by

stubble. The two plots in Grignon were not sown at the same time, so pollen measurements were made at two different flowering dates. Runs were carried out on 12 occasions in Montargis (R1–R12), and 9 ($S_1 9 - S_1 17$) and 15 ($S_2 18 - S_2 32$) occasions in Grignon for the first and second dates, respectively. Measured concentrations and deposition rates of some of the runs used for simulations are given in Table 2.

2.2.2. General framework

The simulated total area was divided in three canopy zones: one located upwind from the maize crop (zone 1), the maize plot (zone 2); and one located downwind from the maize crop (zone 3) (Fig. 1). The maize plot was the only source of pollen. In all simulations, zones 1 and 3 had the canopy characteristics of either bare soil or stubble depending on the chosen experiment location. Only ground deposition was taken into consideration in zones 1 and 3, as the canopies in these zones were short and not dense.

2.2.3. Turbulence

Each field was characterised by: vegetation height, h_c^i (index i denotes the canopy zone); displacement height d_i; its roughness length z_0^i; and leaf area density vertical profile LAD^i. For the maize plots (zone 2), z_0 and d, were taken as $z_0 = 0.1 \times h_c$ and $d_i = 0.7 \times h_c$ (Kaimal and Finnigan, 1994). For zones 1 and 3, z_0^i was estimated by fitting measured and calculated wind profiles as explained below (Table 2). The mean wind speed U_{ref} at the reference height (z_{ref}) was estimated from measured friction velocity $u*$ and Monin–Obukhov length L over the downwind field (zone 3), using Monin–Obukhov similarity theory:

$$U(z) = \frac{u*}{k}\left\{\ln\left(\frac{z-d}{z_0}\right) - \Psi_{\mathrm{m}}\left(\frac{z-d}{L}\right) + \Psi_{\mathrm{m}}(z_0/L)\right\}, \tag{6}$$

where k is the von Kármán constant and ψ_{m} is the stability correction function given by Dyer (1974):

$$\psi_{\mathrm{m}}((z-d)/L) = \begin{cases} \ln\left[\left(\frac{1+x^2}{2}\right)\left(\frac{1+x}{2}\right)^2\right] - 2\,\mathrm{a}\tan x + \frac{\pi}{2} & -2 \leqslant (z-d)/L \leqslant 0 \\ -5.2((z-d)/L) & 0 \leqslant (z-d)/L \leqslant 1 \end{cases} \tag{7}$$

with $x((z-d)/L) = (1 - 16((z-d)/L))^{1/4}$. The stability parameter $(z-d)/L$ is negative when the air stratification is unstable and positive when stable.

Within each canopy, the wind speed profile was defined by $U(z)/U(h_c) = \exp[\gamma(z/h_c - 1)]$ (Cionco, 1972). The attenuation factor, γ, for open canopies ($= 2.5$) was used (Raupach et al., 1996). Measured values of $\sigma_w/u*$, above the canopy, for all experiments

Table 2
Measured concentrations and deposition rates as well as parameters used in the model for each simulation of Fig. 3. z_0 is the roughness length, $u*$ is the friction velocity, and L the Monin–Obukhov length over the downwind surface; U_{ref} is the calculated wind speed at $z = 50$ m over the downwind surface, using the values given in this table for z_0, $u*$ and L

	Concentrations (grains m^{-3})												Deposition rates (grains m^{-2} s^{-1})												z_0 (m)	$u*$ (m s^{-1})	$1/L$ (m^{-1})	U_{ref}(m s^{-1})
	$x = 3$ m						$x = 10$ m																					
	[a]6.4	4	2	1	0.5	0.25	6.4	4	2	1	0.5	0.25	1	2	3	4	8	10	16	32	60	120	200					
R6		34	133	116	116	92		20	22	41	38	34	69	70	54	35	12	8	4	3					0.06	0.21	−0.04	2.57
R7		10	44	46	55	37		5	4	12	13	8	50	20	27	13	10	8	7	5					0.02	0.17	−0.11	2.42
$S_1$13	4	18	62	94	94	102	8	12	28	37	33	36	91	63	52	29	13	11	5	1.2	0.6	0.2	0.2		0.03	0.29	−0.11	3.84
$S_2$21	1	3	27	36	32	30	1	1	5	6	6	6	52	38	29	24	15	6	2		0.2	0.1			0.1	0.31	−0.06	3.5

[a]Height z (m) for concentration and downwind distance x (m) for deposition rates.

were between 1.3 and 1.4, but $\sigma_u/u*$ values changed with the atmospheric stability and wind direction. However, for all simulations, values of $\sigma_u/u* = 3.1$ and $\sigma_w/u* = 1.4$ were used above the canopy under neutral conditions. Stability effects were taken into account as indicated in Loubet (2000). These somehow ideal values were preferred to test the model as measured values may not always be available from field experiments. Values of $u*$ and L^{-1} were measured for each simulation (Table 2).

Over the transition zone, the x_{upwind} and x_{downwind} distances were adjusted to fit measured wind speed profiles at $x = 3$ and 10 m, respectively. They ranged from 3 to $10 \times h_c$, and from 10 to $20 \times h_c$ at the upwind and downwind edge of the source field, respectively.

2.2.4. Canopy structure

The maize LAD(z) profile and its projections along the horizontal and vertical plane (LAD^x and LAD^z) was assumed to have the same shape for Grignon and Montargis. It was based on measurement of the canopy structure in three dimensions made during the Grignon experiment using a digitiser (Fig. 2). A characteristic leaf size (leaf width) was used to estimate pollen deposition on vegetation. To minimise the number of parameters the leaf width was fixed at 0.05 m for maize and 0.01 for bare soil or stubble. The height and size of the tassels (the "source" of pollen) were measured during each experiment and are given in Table 1.

2.2.5. Numerical settings and validation strategy

The number of trajectories, N_p, for each simulation was 10 000. The size of the total area was $z_D = 10$ m, and $x_D = 130$ and 254 m for Montargis and Grignon, respectively. The number of grid divisions was $N_x = 100$ for the horizontal, $N_z = 20$ for the vertical and $N_h = 10$ within the canopy.

During the experiments, the pollen release rate to the atmosphere was not quantified (see Jarosz et al., 2003). However, this variable constitutes a major input of SMOP-2D and needs to be determined. Therefore, the source strength for each simulation was estimated by "inversion" of the model. Similarly to the approach of Aylor and Flesch (2001), the inversion was carried out by first running the model with a release rate of 1 grain $\text{m}^{-2}\,\text{s}^{-1}$ and calculating the concentration profile at 3 m. Measured concentrations were plotted against calculated concentrations and a linear regression with zero intercept was performed. The slope of this regression was taken as the estimation of the actual source strength.

Since the source strength of the model was chosen to make measured and modelled concentrations fit at $x = 3$ m, the quality of the model was validated using measured and calculated deposition rates and vertical concentration profiles at $x = 10$ m.

3. Results

Simulations were done on 8 runs in Montargis, 5 for S_1 and 14 for S_2 in Grignon. Fig. 3 shows vertical profiles of measured and simulated concentrations at $x = 3$ and 10 m and measured and simulated deposition rates downwind from the source plot, for

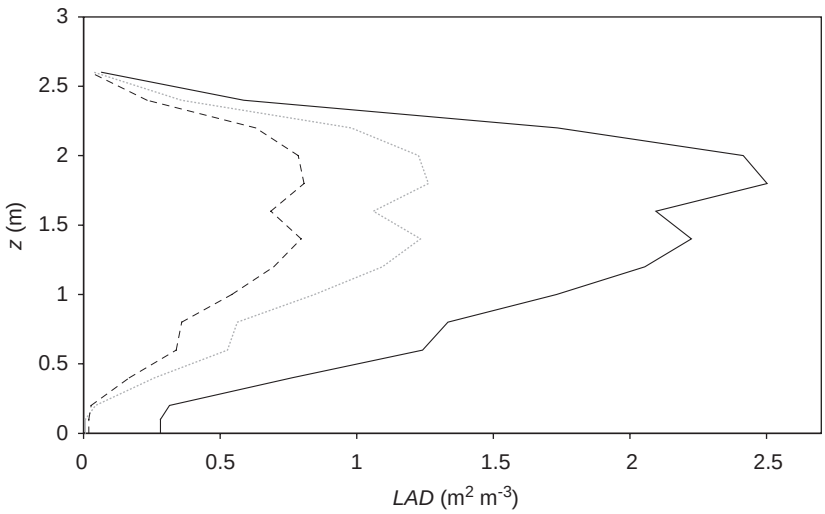

Fig. 2. Profile of leaf area densities (LAD) (bold line) used in the model for Grignon and Montargis. The corresponding LAI was roughly 4. The projection of LAD along the horizontal LAD^x (grey continuous line) and the vertical planes LAD^z (black dotted line) are also represented.

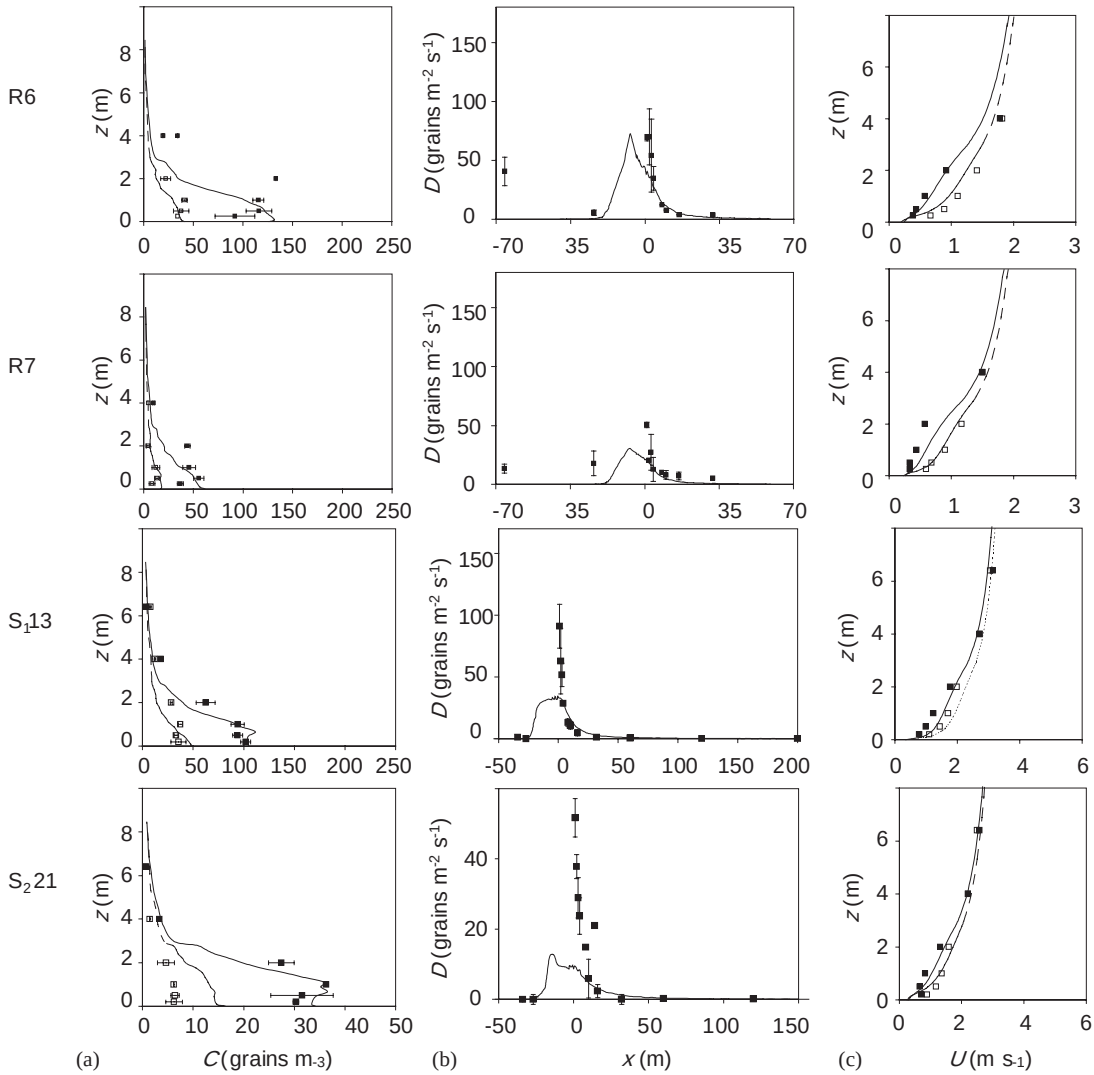

Fig. 3. Results of Montargis and Grignon simulations (R6, R7, $S_1$13, $S_2$21). (a) Measured concentration profile (C) at $x = 3$ m (■) and $x = 10$ m (□) and simulated profiles at $x = 3$ m (thin line) and at $x = 10$ m (dotted line) downwind from the source. (b) Measured (■) and simulated (thin line) deposition downwind from the source (D). (c) Measured profiles of mean wind speed U at $x = 3$ m (■) and $x = 10$ m (□) and simulated at $x = 3$ m (thin line) and at $x = 10$ m (dotted line) downwind from the source.

four representative runs (R6, R7, $S_1$13 and $S_2$21). As the parameters z_0, d, x_{downwind} and x_{upwind} were determined for each run by fitting the measured and simulated vertical profiles of horizontal wind speed at $x = 3$ and 10 m, these profiles are also shown in the figure for the same runs. Concentrations at Grignon were measured to a higher level (at $z = 6.4$ m) and deposition rates were measured further down ($x = 200$ m) than at Montargis.

3.1. Airborne concentration

There was good general agreement between measured and simulated concentration profiles at $x = 3$ and 10 m: the order of magnitude of the concentration at $x = 10$ m is correct, and the shape of the concentration profiles at $x = 3$ and 10 m was reasonably reproduced. However, at $x = 3$ m, the model systematically underestimates the concentrations at heights $z = 2$ and 4 m, the modelled pollen plume settling down too quickly compared to field measurements. Fig. 4 shows the vertical profiles of the mean relative error between measured and modelled concentration (i.e. the difference between the two concentrations divided by the measured concentration). The agreement between the model and the measurements tended to be better for the Grignon runs than those at Montargis. The simulation underestimated the

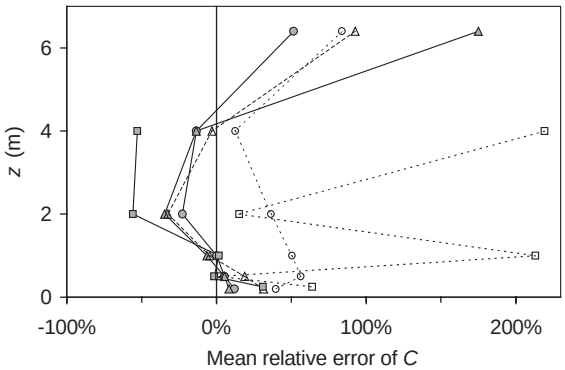

Fig. 4. Mean relative error between measured and modelled concentration in Montargis (□) and Grignon (S1 △, S2 ◯) at $x = 3$ m (thin line) and at $x = 10$ m (dotted line) downwind from the source as a function of height z. First, for each simulation, the relative error was calculated as the difference between measured and simulated deposition divided by measured deposition at a given distance. Then, the relative errors were averaged to produce this graph.

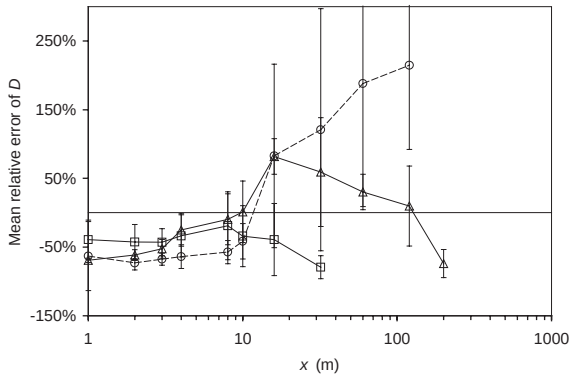

Fig. 5. Mean relative error between measured and modelled deposition rates in Montargis (□) and Grignon (S1 ○, S2 △) at different distances downwind from the source. First, for each simulation, the relative error was calculated as the difference between measured and simulated deposition divided by measured deposition at a given distance. Then, the relative errors were averaged to produce this graph.

2 and 4 m concentrations for the 3 m profile by about 50% at Montargis, but by less than 25% at Grignon. The simulation of the 10 m profile at Montargis overestimated concentration by up to 200% ($z = 1$ and 4 m), while at Grignon errors, for $z \leqslant 4$ m, were usually less than 50%. The better fit at Grignon was probably because the maize plot was larger than in Montargis and completely isolated from other maize pollen sources.

3.2. Deposition rates

The model tended to estimate the order of magnitude of deposition rates relatively well (Fig. 3b). Fig. 5 shows the mean relative error between the simulated and measured deposition rate as a function of the downwind distance to the source. In all cases, deposition rates were underestimated close to the source. For the Montargis runs the deposition rate was always underestimated by approximately 40% for $x \leqslant 16$ m and up to 80% for $x = 32$ m. In contrast to Montargis, for the Grignon runs deposition rates were very well simulated for $x = 8$ m: relative errors were close to zero. But, they were overestimated at distances of 16, 60 and 120 m and underestimated at $x = 200$ m (note that only series S_1 gives measurements for $x = 200$ m).

4. Discussion

In all the simulations presented in this study, the model tended to underestimate pollen deposition rate in the vicinity of the maize plot whereas it correctly simulated the concentration levels. It could be argued that correctly modelling deposition rate near the source is not essential if the object is to determine potential outcrossing, which takes place at larger distances. However, local deposition is a factor in the quantity of pollen available for long-range transport and is therefore important to determine. Various possible explanations are explored below to explain why the model underestimated deposition rates.

4.1. Deposition measurements

Deposition rates may have been influenced by the height at which the measurements were taken (25 and 30 cm high in both sites). To explore this, a simulation was run where all particles were deposited at a height of 30 cm. There were no significant differences between deposition rates at 30 cm and at ground level, suggesting that deposition rates at 0 and 30 cm are identical. This is reasonable since the time spent by the pollen in the layer 0–30 cm is on average equal to $0.3/V_s \sim 1$ s, which is small. It was also thought that the shape of the deposition containers may influence pollen deposition by modifying local turbulence. McCartney and Lacey (1991) have shown that the number of fungal spores collected on horizontal microscope slides openly exposed was almost twice that collected on slides placed on a table or at the bottom of large beakers. Hence, collecting pollen in containers could have led to the underestimation of the deposition rate, although in these experiments the containers were short (less than 7 cm high) compared to those used by McCartney and Lacey (1991) which were 215 mm high. Thus, sampling errors due to the use of containers would be expected to have led to underestimates and not overestimates of deposition rate. Such errors would have made the comparison

with the model worse. Therefore, effects of pollen collector position and shape are unlikely to explain the discrepancy between measurements and simulations.

4.2. Concentration measurements

Another possible explanation for the discrepancy between measurements and the model is an underestimation of the concentration by the rotating-arm pollen traps. This would lead to the underestimation of the source strength and in turn to the underestimation of the deposition rate by the model. If this were the case, the correct concentrations would be higher, and so would the source strength and the predicted deposition rates. However, an increased deposition rate at all distances would not lead to a better fit of the measurements as the model underestimates the deposition rates only near the source (Fig. 4).

4.3. Settling velocity

The underestimation of deposition close to the source could be linked to an erroneous parameterisation of the distribution of settling velocities for maize pollen. In all runs, the distribution of V_s was taken from Di-Giovanni et al. (1995), who found a Gaussian distribution with a mean of $0.31\,\mathrm{m\,s^{-1}}$ and a standard deviation of $0.08\,\mathrm{m\,s^{-1}}$. Observations by one of the authors (Jarosz, 2003), as well as experiments by Aylor (2002), gave a wider range of values for V_s, with generally lower means from 0.20 to $0.32\,\mathrm{m\,s^{-1}}$, with an average of $0.26\,\mathrm{m\,s^{-1}}$. However, using a smaller value of V_s would increase underestimation of deposition rate by the model. Indeed, it is generally thought that heavier pollen or clusters settle more quickly than single pollen grains. Clusters of maize pollens with 2 or 3 pollen grains have been observed in laboratory experiments by Ferrandino and Aylor (1984), Di-Giovanni et al. (1995), and Aylor (2002), although such clusters have not been reported in the field. Ferrandino and Aylor (1984) have reported that maize pollen doublets and triplets settle 40% and 73% faster than single pollen grains, respectively. The model assumed that all pollen grains were single. To examine the underestimation of settling velocity, the model was run for different sized clusters of pollen grains. The settling velocity of a cluster of N maize pollen grains has been shown to be $V_s^N = V_s\sqrt{N}$ (Ferrandino and Aylor, 1984), giving $V_s^2 = 0.37\,\mathrm{cm\,s^{-1}}$ and $V_s^3 = 0.45\,\mathrm{cm\,s^{-1}}$ for doublets and triplets, respectively. Fig. 6 shows the concentration profiles and the deposition rates simulated for run $S_1 13$, with V_s ranging from that for single pollen to a cluster of 5 grains (which are unlikely to exist). The model simulated deposition rates near the source better for higher V_s but did not correctly simulate the concentration profiles, especially at $x = 10\,\mathrm{m}$, where measured concentrations were greatly underestimated for high values of V_s. The hypothesis of a mixed population of single grains and clusters of pollen can be evaluated based upon Fig. 6. Since concentration and deposition rate are proportional to the source strength, for a mixed population of pollen, they would simply be a weighed sum of each cluster's concentrations and deposition rates. Therefore, the behaviour of the model remains the same for mixed population as for unmixed ones. These results suggest that it is unlikely that the errors in pollen settling velocity and/or the effects of clusters are solely responsible for the underestimation of deposition by the model near the source.

4.4. Pollen resuspension

Pollen resuspended from the ground, or from vegetation, could have contributed to the pollen deposit, hence increasing the measured deposition rates close to the source . Aylor et al. (2003) have shown experimentally that pollen could be quite easily dislodged from maize leaves by either leaf shaking, roll-off or light air flow

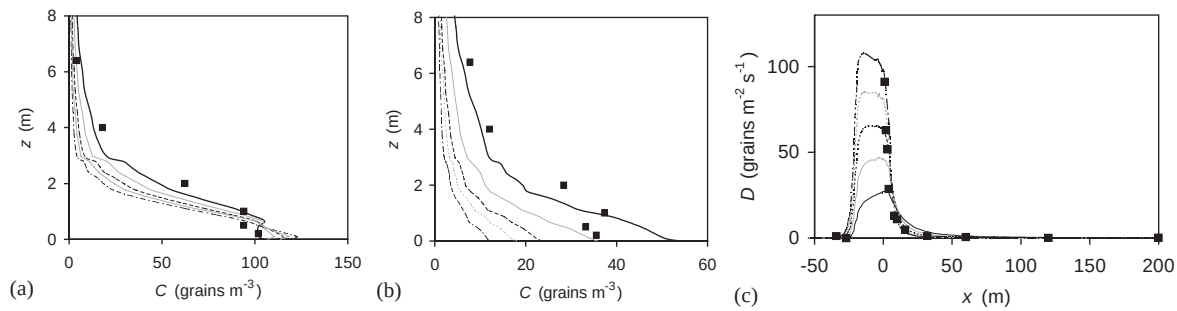

Fig. 6. Sensitivity analysis of the settling velocity V_s. Concentration profile at (a) $x = 3\,\mathrm{m}$ and (b) $x = 10\,\mathrm{m}$ downwind from the source and (c) the deposition as a function of x are represented for simulations $S_1 13$ with $V_s = 0.26\,\mathrm{m\,s^{-1}}$ for single grains (black thin line), $0.37\,\mathrm{m\,s^{-1}}$ for doublets (grey thin line), $0.45\,\mathrm{m\,s^{-1}}$ for triplets (black dotted line), $0.52\,\mathrm{m\,s^{-1}}$ for quadruplets (grey dotted line) and $0.58\,\mathrm{m\,s^{-1}}$ for quintuplets (black dotted dash line).

(0.2–0.5 m s^{-1}). They have also shown that maize pollen does not stick to leaf hairs. Resuspension has also been observed for other particles in the laboratory (Aylor and Ferrandino, 1985; Braaten et al., 1990; Ibrahim et al., 2003). Thus, pollen resuspension from leaves is likely to occur in the field. Simulations (not shown) were performed with pollen sources at two different heights, 1.7 and 2.0 m, corresponding to the height of maximum observed LAD in the crop. Two values of V_s were also used: $V_s = 0.26\,\mathrm{m\,s^{-1}}$, which corresponds to fresh pollen and $V_s = 0.15\,\mathrm{m\,s^{-1}}$, which corresponds to dry pollen (Jarosz, 2003). These sources represented pollen from potential resuspension sites in the maize plot. None of these simulations enhanced the agreement between simulated and measured deposition rates close to the source, suggesting that the discrepancy could not readily be explained by the resuspension of pollen from the crop.

4.5. Effect of the β parameter

Wilson (2000) reported simulations of the deposition of glass beads (mean diameter $\varnothing = 107\,\mu\mathrm{m}$) released from a point source at 15 m high over prairie land. He found that β had a great influence on the deposition rates. We ran simulations (not shown) with different values of β ($\beta = 1.5$, 2, 3, 4 and 5). They showed little influence of β on short-range deposition of pollen. Increasing β seemed to decrease vertical diffusion near the source but also to decrease deposition further downwind.

4.6. Turbulence

Another possible cause of the model's underestimation of deposition close to the source lies in the difficulty to correctly describe the turbulent flow in the transition zone at the downwind edge of the source, especially for U, W, σ_w and $\overline{u'w'}$. For example, higher turbulence intensities would induce higher vertical diffusion, which would favour larger deposition rates near the source and increased concentration above the source level.

The topography at Montargis and Grignon was especially complex, and the area downwind from the source could not be considered as a simple rough to smooth transition zone. The maize canopies were only about 20 m long on the downwind side ($\sim 10\ h_c$), hence the area downwind from the source was still under the influence of the smooth to rough transition zone of the upwind edge (Irvine et al., 1997). Measurements of turbulence intensities downwind from the plots, using ultrasonic anemometers (Gill, R2 and R3, data not shown), gave an increase in $\sigma_w/u*$ over the standard boundary layer value ($\sim 1.7\,u*$ instead of $1.3\,u*$) in the first 10 m downwind from the maize plot. Moreover, W measured downwind from the canopy showed a marked downward flow ($W \sim -0.7\ u*$), whereas the parameterisation used gave $W \sim -0.4\ u*$. These observations are in good agreement with Irvine et al. (1997) for $x/h_c = 14.5$ downwind from a smooth to rough edge, which corresponds to $x = 10$–15 m in our study. Hence, enhanced σ_w and negative W near the source could partly explain higher measured deposition rates, because a negative W directly adds up to the settling velocity, and an enhanced σ_w induces a larger diffusive flux (upward but also downward), and hence a larger deposition rate near the source. Further downwind, the deposition may be reduced by a larger σ_w due to the depletion near the source. Parameterised values of $\overline{u'w'}$ were much lower in absolute value (by a factor of 2 to 3) than those measured over the canopy and downwind ($\overline{u'w'}\ \sim -4\,u*^2_{\mathrm{upwind}}$). Irvine et al. (1997) found an increase of up to $-2.5\,u*^2$ downwind from a single transition. In the model, higher $\overline{u'w'}$, like higher σ_w, would tend to both increase upward dispersion and downward diffusion, and therefore deposition. However, the underestimation of $\overline{u'w'}$ in the model was probably much higher than the underestimation of σ_w. Consequently, it is likely that a better parameterisation of $\overline{u'w'}$, W and σ_w for the transition zone in the model would result in increased agreement between predicted and measured deposition rates near the source.

5. Conclusion

This study shows that SMOP-2D correctly simulated the airborne pollen concentration pattern downwind from a small-sized maize crop but generally underestimated the deposition rates in the first 10 m downwind from the crop. Factors that could account for the discrepancy between modelled and measured deposition rates were evaluated by sensitivity analysis. This analysis led to the conclusion that the underestimated deposition rates were probably not due to: (1) biased concentration or deposition rate measurements, (2) presence of heavier pollen, or clusters of pollens, with higher V_s, (3) pollen resuspension from leaves in the plot or the ground, or (4) a wrong value of the β parameter reducing the particle Lagrangian time scale. The analysis suggests that model underestimation of the deposition rate was more likely due to the incorrect parameterisation of the turbulent field over and close to the emitting source. This highlights the need for Lagrangian Stochastic models to be coupled with at least second-order Eulerian flow models if they are to be used for complex terrain.

Many processes apart from pollen dispersal are also involved in outcrossing in maize crops. For example, biological factors such as pollen viability, silk receptivity, synchronisation of timing of flowering between crops, and competition between foreign and local pollen. Outcrossing can also be affected by other meteorological

factors, including rain wash out and ultra violet solar radiation (affecting pollen viability). Thus models trying to estimate outcrossing would require either mechanistically or empirically integrating all these features.

Acknowledgements

Many thanks to Jean Louis Drouet for numerically rebuilding the 3D maize structure. We also thank Alastair McCartney for his helpful comments on this paper and Suzette Tanis-Plant for editorial advice. This work was funded by INSU/CNRS, Convention No 01 CV 081, as well as by INRA (Institut National de la Recherche Agronomique), FNPSMS (Fédération Nationale de la Production des Semences de Maïs et Sorgho) and GNIS (Groupement National Interprofessionel des Semences et plants).

References

Aylor, D.E., 2002. Settling speed of corn (*Zea mays*) pollen. Journal of Aerosol Science 33, 1601–1607.

Aylor, D.E., Ferrandino, F.J., 1985. Rebound of pollen and spores during deposition on cylinders by inertial impaction. Atmospheric Environment 19 (5), 803–806.

Aylor, D.E., Flesch, T.K., 2001. Estimating spore release rates using a lagrangian stochastic simulation model. Journal of Applied Meteorology 40, 1196–1208.

Aylor, D.E., Schultes, N.P., Shields, E.J., 2003. An aerobiological framework for assessing cross-pollination in maize. Agricultural and Forest Meteorology 119, 111–129.

Baltazar, B.M., Schoper, J.B., 2002. Crop-to-crop gene flow: dispersal of trangenes in maize, during field tests and commercialization. Proceedings of the Seventh International Symposium on the Biosafety of Bioengineered Organisms, Beijing, China.

Braaten, D.A., Paw, U.K.T., Shaw, R.H., 1990. Particle resuspension in a turbulent boundary layer-observed and modeled. Journal of Aerosol Science 21 (5), 613–628.

Bradley, E.F., 1968. A micrometeorological study of velocity profiles and surface drag in the region modified by a change in surface roughness. Quaterly Journal of the Royal Meteorological Society 94, 361–379.

Cionco, R., 1972. A wind-profile index for canopy flow. Boundary-Layer Meteorology 3, 255–263.

Di-Giovanni, F., Kevan, P.G., Nasr, M.E., 1995. The variability in settling velocities of some pollen and spores. Grana 34, 39–44.

Doebley, J., 1990. Molecular evidence for gene flow among Zea species Genes transformed into maize through genetic engineering could be transferred to its wild relatives, the Teosintes. Bioscience 40, 443–448.

Dyer, A.J., 1974. A review of flux-profile relationships. Boundary-Layer Meteorology 7, 363–372.

Ferrandino, F.J., Aylor, D.E., 1984. Settling speed of clusters of spores. Ecology and Epidemiology 74 (8), 969–972.

Flesch, T.K., 1995. The footprint for flux measurements, from backward lagrangian stochastic models. Boundary-Layer Meteorology 78, 399–404.

Ibrahim, A.H., Dunn, P.F., Brach, R.M., 2003. Microparticle detachment from surfaces exposed to turbulent air flow: controlled experiments and modeling. Journal of Aerosol Science 34, 765–782.

Irvine, M.R., Gardiner, B.A., Hill, M.K., 1997. The evolution of turbulence across a forest edge. Boundary-Layer Meteorology 84, 491–496.

Jackson, S.T., Lyford, M.E., 1999. Pollen dispersal models in Quaternary plant ecology: assumptions, parameters, and prescriptions. The Botanical Review 65 (1), 39–75.

Jarosz, N., 2003. Etude de la dispersion atmosphérique du pollen de maïs. Contribution à la maîtrise des risques de pollinisation croisée. Ph.D. Thesis, Institut National Agronomique de Paris-Grignon, France, 125 pp.

Jarosz, N., Loubet, B., Durand, B., McCartney, H.A., Foueillassar, X., Huber, L., 2003. Field measurements of airborne concentration and deposition of maize pollen. Agricultural and Forest Meteorology 119 (1–2), 37–51.

Kaimal, J.C., Finnigan, J.J., 1994. Atmospheric boundary layer flows, their structure and measurement. Oxford University Press, Oxford, 283 pp.

Klein, E., 2000. Estimation de la fonction de dispersion du pollen. Application á la dissémination de trangènes dans l'environnement. Ph.D. Thesis, University of Paris Sud, France, 80 pp.

Lavigne, C., Klein, E.K., Vallée, P., Pierre, J., Godelle, B., Renard, M., 1998. A pollen dispersal experiment with transgenic oilseed rape. Estimation of the average pollen dispersal of an individual plant within a field. Theoretical and Applied Genetics 96 (6/7), 886–896.

Legg, B.J., Powell, F.A., 1979. Spore dispersal in a barley crop: a mathematical model. Agricultural Meteorology 20, 47–67.

Leuzzi, G., Monti, P., 1998. Particle trajectory simulation of dispersion around a building. Atmospheric Environment 32 (2), 203–214.

Loubet, B., 2000. Modélisation du dépôt sec d'ammoniac atmosphérique à proximité des sources. Ph.D. Thesis, University of Toulouse, France, 330 pp.

Matsuoka, Y., Vigouroux, Y., Goodman, M.M., Sanchez, J., Buckler, E., Doebley, J., 2002. A single domestication for maize shown by multilocus microsatellite genotyping. Proceedings of the National Academy of Sciences 99, 6080–6084.

McCartney, H.A., Bainbridge, A., Stedman, O.J., 1985. Spore deposition velocities measured over a barley crop. Phytopathology 114, 224–233.

McCartney, H.A., Lacey, M.E., 1991. Wind dispersal of pollen from crops of oilseed rape (*Brassica napus* L.). Journal of Aerosol Science 22 (4), 467–477.

Raupach, M.R., Finnigan, J.J., Brunet, Y., 1996. Coherent eddies and turbulence in vegetation canopies: the mixing-layer analogy. Boundary-Layer Meteorology 78, 351–382.

Reynolds, A.M., 1999. A lagrangian stochastic model for heavy particle deposition. Journal of Colloid and Interface Science 215, 85–91.

Rodean, H.C., 1996. Stochastic Lagrangian Models of turbulent Diffusion. Meteotological Monographs, vol. 26(48) American Meteorological Society, Boston, USA, 84 pp.

Sawford, B.L., Guest, F.M., 1991. Lagrangian statistical simulation of the turbulent motion of heavy particles. Boundary-Layer Meteorology 54, 147–166.

Snyder, W.H., Lumley, J.L., 1971. Some measurements of particle velocity autocorrelation functions in a turbulent flow. Journal of Fluid Mechanics 48 (I), 41–71.

Thomson, D.J., 1987. Criteria for the selection of stochastic models of particle trajectories in turbulent flows. Journal of Fluid Mechanics 180, 529–556.

Walklate, P.J., 1986. A markov-chain particle dispersion model based on air flow data: extension to large water droplets. Boundary-Layer Meteorology 37, 313–318.

White, S., Doebley, J., 1998. Of genes and genomes and the origin of maize. Trends in Genetics 14, 327–332.

Wilson, J.D., 2000. Trajectory models for heavy particles in atmospheric turbulence: comparison with observations. Journal of Applied Meteorology 39, 1894–1912.

Wilson, J.D., Flesch, T.K., 1997. Trajectory curvature as a selection criterion for valid lagrangian stochastic dispersion models. Boundary-Layer Meteorology 84, 411–425.

Wilson, J.D., Sawford, B.L., 1996. Review of lagrangian stochastic models for trajectories in the turbulent atmosphere. Boundary-Layer Meteorology 78, 191–210.